HHS Public Access

Author manuscript

*Biochem J*. Author manuscript; available in PMC 2015 June 18.

Published in final edited form as:

*Biochem J*. 2013 June 1; 452(2): 293–301. doi:10.1042/BJ20130025.

# Molecular Orientation of Factor VIIIa on the Phospholipid Membrane Surface Determined by Fluorescence Resonance Energy Transfer

**Hironao Wakabayashi** and **Philip J. Fay**[1]

Department of Biochemistry and Biophysics, University of Rochester School of Medicine, 601 Elmwood Ave., Rochester, NY 14642, USA

## SYNOPSIS

Factor VIIIa (FVIIIa) binds to phospholipid membranes during formation of the FXase complex. Free thiols of Cys residues of isolated FVIIIa A1 and A2 subunits and the A3 domain of A3C1C2 subunit were labeled with PyMPO or fluorescein (fluorescence donors). Double mutants in the A3 domain (Cys2000Ser/Thr1872Cys and Cys2000Ser/Asp1828Cys) were also produced to utilize Cys1828 and Cys1872 residues for labeling. Labeled subunits were reacted with complementary non-labeled subunits to reconstitute FVIIIa. Octadecylrhodamine incorporated into phospholipid vesicles was used as an acceptor for distance measurements between FVIII residues and membrane surface by fluorescence resonance energy transfer. Results indicated that a FVIII axis on a plane that intersects the approximate center of each domain is oriented with a tilt angle of ~30–50° on the membrane surface. This orientation predicted the existence of contacts mediated by residues 1713-1725 in the A3 domain in addition to a large area of contacts within the C domains. FVIII variants where residues Arg1719 or Arg1721 were mutated to Asp showed a >40-fold reduction in membrane affinity. These results identify possible orientations for FVIIIa bound to the membrane surface and support a new interaction between the A3 domain and membrane likely mediated, in part by Arg1719 and Arg1721.

### Keywords

factor VIII; phospholipid membranes; protein structure; fluorescence resonance energy transfer; blood coagulation

## INTRODUCTION

Factor (F)VIII is a plasma protein that is decreased or defective in individuals with hemophilia A. FVIII circulates as a heterodimer consisting of a heavy chain (HC) comprised of A1, A2 and B domains and a light chain (LC) comprised of A3, C1 and C2 domains (see Ref. [1] for review). FVIII is activated following limited proteolysis catalyzed by thrombin

[1]To whom correspondence should be addressed: Philip J. Fay, Department of Biochemistry and Biophysics PO box 712, 601 Elmwood Ave., Rochester, NY 14642. Tel: 585-275-6576. Fax: 585-275-6007; philip_fay@urmc.rochester.edu.

**AUTHOR CONTRIBUTION**

Hironao Wakabayashi designed and performed the experiments, analyzed the data and wrote the manuscript. Philip J. Fay contributed to the direction and design of the study, and preparation of the manuscript.

or FXa to yield FVIIIa, a heterotrimer comprised of subunits designated A1, A2, and A3C1C2, that functions as a cofactor for FIXa in the membrane-dependent activation of FX to FXa (see Ref. [1] for review).

The intermediate resolution X-ray structures of FVIII [2, 3] showed that the C1 and C2 domains are aligned such that both domains may interact with the phospholipid membrane vesicle (PLV) surface and with close contact between A1 and C2 domains. Binding of FVIIIa to PLV is essential for cofactor function and maximal FXase activity [4]. This binding requires negative charge provided from stereospecific phosphatidyl-L-serine [4, 5] and the presence of both C1 and C2 domains for optimal interaction [6].

Membrane binding regions have been identified in the C2 domain and include Leu2251-Leu2252, Met2199-Phe2200, Lys2227, and Trp2313-His2315 [7–10]. We reported that a FVIII variant lacking the C2 domain retained the capacity to bind PLV, albeit with a marked reduction in affinity [11], supporting a direct role for the C1 domain in this interaction. More recent mutagenesis studies identified sites for PLV binding in C1 including Lys2092-Phe2093 [12], Gln2042-Tyr2043, and Arg2159 [13]. Furthermore, homologous sites in FVa C1 and C2 domains have been reported to be important for PLV binding and include Tyr1956-Leu1957, Arg2023-Arg2027 [14], and Trp2063-Trp2064 [15, 16], which correspond to FVIII sites Lys2092-Phe2093, Arg2159-Arg2163, and Met2199-Phe2200, respectively. Most of these PLV binding residues are located at spikes near the tips of the C1 and C2 domains, except for Trp2313-His2315 which is on a flanking side of C2 domain [10].

In the current study we utilized a donor fluorophore labeling a single free thiol on a FVIIIa subunit and an acceptor fluorophore distributed on the PLV. Those donor sites include Cys310, Cys692, or Cys2000 in each FVIII A domain. In addition Cys1828 and Cys1872 in A3 domain were utilized following preparation of the double mutants (Cys2000Ser/Asp1828Cys and Cys2000Ser/Thr1872Cys). FVIIIa was reconstituted from purified subunits (A1, A2, and A3C1C2) containing a single labeled subunit plus the unlabeled complement. Results from distance calculations using multiple point measurements as determined by fluorescence resonance energy transfer (FRET) identify the molecular orientation of FVIIIa relative to the PLV surface.

## EXPERIMENTAL PROCEDURES

### Materials

Recombinant FVIII (Kogenate™) was a generous gift from Dr. Lisa Regan of Bayer Corporation (Berkeley, CA). Dioleoyl phospholipids [Phosphatidylcholine (PC), phosphatidylethanolamine (PE), and phosphatidylserine (PS)] were purchased from Avanti Polar Lipids (Alabaster, AL). Octadecylrhodamine (OR), 1-(2-maleimidylethyl)-4-(5-(4-methoxyphenyl)-oxazol-2-yl)pyridinium methanesulfonate (PyMPO maleimide), and fluorescein-5-maleimide were purchased from Life Technologies (Grand Island, NY). The reagents α-thrombin, FIXa, FX, and FXa (Enzyme Research Laboratories, South Bend, IN), hirudin (DiaPharma, West Chester, OH), and the chromogenic Xa substrate, Pefachrome Xa

(Pefa-5523, $CH_3OCO$-D-CHA-Gly-Arg-pNA·AcOH; Centerchem Inc. Norwalk, CT) were purchased from the indicated vendors.

### Construction and expression of FVIII WT and variants

FVIII variants with the point mutations Arg1719Asp and Arg1721Asp, and the double mutants Cys2000Ser/Asp1828Cys and Cys2000Ser/Thr1872Cys were prepared as B-domainless FVIII (lacking residues Gln744-Ser1637 in the B-domain) [17] using methods previously described [18]. Protein yields for the variants ranged from >10 to ~100 μg from two 750 $cm^2$ culture flasks, with purity >90% as judged by SDS-PAGE. The primary contaminant in the FVIII preparations was albumin. FVIII concentrations were measured using an ELISA and FVIII activity was determined by one-stage clotting and two-stage chromogenic FXa generation assays described below.

### FVIIIa subunit purification

A1, A2, and A3C1C2 subunits were purified from Kogenate FVIII following activation by thrombin as described previously [19]. A3C1C2 subunits from Cys2000Ser/Asp1828Cys and Cys2000Ser/Thr1872Cys FVIII were purified according to the following method. Each FVIII variant (1–3 μM) was reacted with thrombin (20 nM) in 20 mM HEPES, pH 7.2, 0.1 M NaCl, 0.01% Tween 20 (buffer A) for 30 min followed by an additional 30 min incubation with another 20 nM thrombin and the reaction sample was treated with 50 mM EDTA overnight at 4°C. After a 1:4 dilution with buffer A, the samples were loaded on a heparin Sepharose column (1.5 cm × 0.7 cm in diameter, GE Healthcare, Piscataway, NJ). After washing with buffer A the bound material (A2 and A3C1C2 subunits) were eluted by 20 mM HEPES, pH 7.2, 0.8 M NaCl, 0.01% Tween 20 (buffer B). This fraction was then applied to a column of R8B12 antibody (GMA8012, Green Mountain Antibodies, Burlington, VT) conjugated to Affigel-10 (Bio-Rad, Hercules, CA) by incubation overnight at 4°C to adsorb the A2 subunit. The unbound fraction was diluted (1:4) with 40 mM 10 mM MES pH 6.0, 0.01% Tween 20 and A3C1C2 subunit was further purified with a Mono S column (GE Healthcare) using a BioLogic DuoFlow system (Bio-Rad) employing a 0–0.8 M NaCl gradient at a flow rate of 1 ml/min. The final A3C1C2 product was >95% pure as judged by SDS-PAGE.

### ELISA

A sandwich ELISA was performed as previously described [20] using purified commercial recombinant FVIII (Kogenate, Bayer Corporation) as a standard. FVIII capture used the anti-C2 monoclonal antibody (GMA8003, Green Mountain Antibodies) and the anti-A2 monoclonal antibody, R8B12 was employed for FVIII detection following biotinylation.

### One-stage clotting assay

One-stage clotting assays were performed using substrate plasma chemically depleted of FVIII [21] and assayed using a Diagnostica Stago clotting instrument. Plasma was incubated with APTT reagent (Trinity Biotech USA Inc., Jamestown, NY) for 6 min at 37°C after which a dilution of FVIII was added to the cuvette. After 1 min the mixture was recalcified, and clotting time was determined and compared to a pooled normal plasma standard.

### Two-stage chromogenic FXa generation assay

The rate of conversion of FX to FXa was monitored in a purified system [22] according to methods previously described [23, 24]. The specific activity of each FVIII variant was assessed under conditions where FIXa was saturated by FVIIIa. FVIII (40 nM) in 20 mM HEPES, pH 7.2, 0.1 M NaCl, 0.01% Tween 20, 0.01% BSA, 5 mM $CaCl_2$ (HEPES buffer) containing 20 μM PS:PC:PE vesicles was activated with 20 nM α-thrombin for 1 min. The reaction was stopped by adding hirudin (10 U/ml) and the resulting FVIIIa was reacted with FIXa (0.3 nM) for 1 min. FX (300 nM) was added to initiate reactions which were quenched after 1 min by the addition of 50 mM EDTA. FXa generated was determined following reaction with the chromogenic substrate Pefachrome Xa (0.46 mM final concentration). All reactions were run at 23°C.

### PLV preparation

PLV (large unilamellar vesicles) containing 20% PC, 50% PE, and 30% PS (or 100% PC) were prepared using octylglucoside as described previously [25] and phospholipid concentration was determined by an inorganic phosphorus assay [26]Several PLV materials containing various concentration of OR were prepared by mixing 10 mg PC:PE:PS and 0.1–1.2 mg OR in 1 mL chloroform and processed as described [27]. Phospholipid concentration was determined by method as described [25] and OR concentration was determined by absorbance at 564 nm (molar extinction coefficient = 95,400 $M^{-1}cm^{-1}$). The number of OR molecules per unit phospholipid area ($\sigma$) was estimated to be $1.25 \times 10^{-4} – 1.76 \times 10^{-3}$ OR molecules/$Å^2$ based on the criterion that each phospholipid occupies an area of 70 $Å^2$ [27].

### Fluorophore labeling of FVIII and FVIIIa subunits

FVIII (WT, Arg1719Asp, and Arg1721Asp), A1, or A3C1C2 (WT, Cys2000Ser/Asp1828Cys, or Cys2000Ser/Thr1872Cys) subunit were labeled with PyMPO maleimide (excitation max/emission max = 417 nm/550 nm) as described [11, 23] or fluorescein-5-maleimide (excitation max/emission max = 495 nm/520 nm) using a 20-fold molar excess of PyMPO maleimide or fluorescein-5-maleimide over FVIII (subunit) and incubated 1 hour at 23°C. Donor fluorophore (PyMPO or fluorescein) labeled A2 was purified from labeled WT FVIII as described previously [19]. Labeling efficiency was determined by comparing the fluorescence intensity with the value of 5 μM PyMPO maleimide or fluorescein-5-maleimide saturated by each 20 μM FVIII subunit and the efficiency values were >0.9 in all cases.

### Reconstitution of FVIIIa

FVIIIa reconstitution using donor fluorophore-labeled A3C1C2 purified from WT, Cys2000Ser/Asp1828Cys, or Cys2000Ser/Thr1872Cys plus unlabeled A1 and A2 was performed by mixing 20 or 40 nM donor fluorophore-labeled A3C1C2 with 1 μM A1 subunit at 37°C for 2 hrs followed by an incubation with A2 subunit (400 nM) for 1 hr at 23°C in HEPES buffer containing 300 μM PC vesicles to prevent non-specific binding. FVIIIa reconstitution using donor fluorophore-labeled A1 plus unlabeled A2 and A3C1C2 was performed by mixing 40 nM donor fluorophore-labeled A1 with 1 μM A3C1C2 subunit at 37°C for 2 hrs followed by an incubation with A2 subunit (400 nM) for 1 hr at 23°C in

HEPES buffer containing 300 μM PC vesicles. FVIIIa reconstitution using donor fluorophore-labeled A2 plus unlabeled A1 and A3C1C2 was done by mixing 1 μM A1 with 2 μM A3C1C2 subunit at 37°C for 2 hrs followed by an incubation with donor fluorophore-labeled A2 subunit (40 nM) for 1 hr at 23°C in HEPES buffer containing 300 μM PC vesicles.

### FVIIIa binding to PLV as measured by FRET

Binding of reconstituted FVIIIa or FVIII (Arg1719Asp or Arg1721Asp) to PLV was monitored by donor (PyMPO or fluorescein) emission quenching resulting from energy transfer to the acceptor (OR) as described [27]. Briefly, 3 titrations were performed including one where labeled FVIIIa/FVIII was titrated with PLV without OR (sample-0), a labeled FVIIIa/FVIII titrated with PLV containing OR (sample-1), and an unlabeled FVIIIa/FVIII titrated with PLV containing OR (sample-2). After addition of PLV, samples were incubated for 10 min prior to determining fluorescence using an Aminco-Bowman Series 2 Luminescence Spectrometer (Thermo Spectronic, Rochester, NY). Wavelength values for PyMPO were 417 nm (excitation, bandwidth: 4 nm) and 540–546 nm (scanned emission, bandwidth 8 nm) and values for fluorescein were 495 nm (excitation, bandwidth: 4 nm) and 520–526 nm (scanned emission, bandwidth 8 nm). After background fluorescence correction, the actual fluorescence after quenching by OR ($F$) was calculated by subtracting sample-2 fluorescence ($F_2$) from sample-1 fluorescence ($F_1$). Relative fluorescence ($F/F_0$) which is the ratio of $F$ to control sample-0 fluorescence ($F_0$) was plotted against phospholipid concentration.

### Calculation of energy transfer parameters

Energy transfer parameters as originally described by Marsh and Lowry [28] were calculated according to previously described methods [29]. Transfer efficiency was determined using the equation.

$$R_0^6 = (8.79 \times 10^{-5}) k^2 n^{-4} Q_D J_{DA}$$

where $R_0$ is the distance at which efficiency of transfer is 50%. $Q_D$ is the quantum yield of the donor fluorophore (PyMPO or fluorescein) in the absence of acceptor fluorophore (OR) that was determined using a quantum yield of quinine sulfate (= 0.7) in 0.1 M $H_2SO_4$ as a standard. In the case of fluorescein, a quantum yield value of disodium fluorescein (= 0.925) in 0.1 M NaOH [30] was used as a standard. The parameter $k^2$ is a geometric factor (= 2/3), n is the refractive index of the medium (1.33), and $J_{DA}$ is the spectral overlap in $M^{-1}cm^{-1}nm^4$ calculated as follows.

$$J_{DA} = \int_0^\infty F(\lambda)\varepsilon_A(\lambda)\lambda^4 d\lambda / \int_0^\infty F(\lambda) d\lambda$$

where $F(\lambda)$ is the corrected net emission intensity at given wavelength, $\varepsilon(\lambda)$ is the molar extinction coefficient of OR at the wavelength in the phospholipid vesicle in the presence of excess unlabeled FVIII.

The values of $Q_{DA}/Q_D$, the ratio of donor quantum yield in the sample with OR-labeled and unlabeled PLV and given by the ratio of the corrected fluorescence intensity of the samples with OR-labeled and unlabeled PLV ($=F/F_0$) under the conditions of an excess concentration of PLV (60 μM), were determined for several OR-PLV preparations with various $\sigma$. Using these sets of data the distance of closest approach ($L$) between the plane of donor fluorophore and the plane of acceptor fluorophore at the outer surface of the phospholipid bilayer was obtained by nonlinear least-squares regression by numerically integrating the following equation [31, 32],

$$Q_{DA}/Q_D = \left(1/\tau_D\right) \int_0^\infty e^{-t/\tau_D}\, e^{-\sigma S(t)} dt$$

with $S(t) = \int_L^\infty \left[1 - e^{-\left(t/\tau_D\right)\left(R_0/R\right)^6}\right] 2\pi R dR$ where $\tau_D$ is the fluorescence lifetime of the donor, $t$ is the time, and $R$ is the distance between the donor and an acceptor.

## Calculation of matching planes from distance data

We initially calculated the possible location of the transition dipole of the donor fluorophore (PyMPO or fluorescein). Based on the chemical structures, points that were 10–20 Å (PyMPO) or 5–15Å (fluorescein) away from the sulfur atom of each Cys residue were selected at 1Å increments. Among the selected points, any that would cause a steric clash with any FVIII atoms were eliminated (assuming the center of transitional dipole of donor fluorophores needed to be at least 3 Å from any FVIII atom). In the case of the Asp1828Cys and Thr1872Cys mutants, the minimum energy rotamer coordinates for the Cys mutations were calculated by Swiss PDB viewer (DeepView, http://spdbv.vital-it.ch/) and the sulfur atom coordinates of the Cys residues were obtained. Subsequently, all possible plane coordinates ($ax + by + cz + d = 0$) (obtained by changing polar coordinates of a plane normal vector with a change of $d$ values) were screened and selected by the following criteria. When the plane satisfied the conditions that for all donor fluorophore sites (PyMPO and fluorescein at amino acid residue 310, 692, 2000, 1828, and 1872) a calculated distance value between the plane and any possible location of transition dipole would fall within the range of the distance ($L$).

## Fluorescence anisotropy

Fluorescence anisotropy was measured using an Aminco-Bowman Series 2 Luminescence Spectrometer in L-format. A sample FVIIIa preparation was made by mixing 200 nM fluorophore-labeled subunits with 1 μM non-labeled subunits (ex. 200 nM PyMPO-labeled A3C1C2 with 1 μM A1 and 1 μM A2 subunits) in 60 μM PLV. Wavelength values for

PyMPO were 417 nm (excitation, bandwidth: 4 nm) and 543 nm (emission, bandwidth 8 nm) and values for fluorescein were 495 nm (excitation, bandwidth: 4 nm) and 523 nm (emission, bandwidth 8 nm). The fluorescence values for all polarizer positions were corrected by subtracting blank values and anisotropy values were calculated as an average of 6 measurements.

### Data analysis

Factor VIII - phospholipid binding kinetics used the following equation:

$$(F/F_0)=1-\frac{Q_{\max}}{A}\cdot\frac{(A+K_d+X/n)^2-\sqrt{(A+K_d+X/n)^2-4AX/n}}{2}$$

where $F/F_0$ is relative fluorescence, $A$ is the concentration of FVIII (25 nM), $X$ is the concentration of phospholipid vesicles, $K_d$ is a dissociation constant, $n$ is a ratio of binding stoichiometry (phospholipid: FVIII), and $Q_{max}$ is the maximum quenching value. The value of $n$ (= 100) was estimated as described previously [11]. Computation for nonlinear least-squares regression analysis was performed using standard curve-fitting algorythm (Gauss-Newton algorythm with Levenberg-Marquardt method).

## RESULTS

### Binding of reconstituted FVIIIa to PLV as determined by FRET

Isolated subunits of FVIIIa labeled at single sites with donor fluorophores were incubated with excess concentrations of the complementary, unlabeled subunits to reconstitute FVIIIa. We have previously utilized Cys310 in A1, Cys692 in A2, and Cys2000 in A3 for fluorophore labeling (see ref [23]), inasmuch as these residues represent the only free Cys residues in each of the three A domains. Thus modification of these free thiol groups is facile, results in minimal change to FVIII structure, and has little if any effect on biologic activity. Two additional A3 domain residues, Asp1828 and Thr1872 were chosen by their location to help distinguish between an upright versus a tilted orientation of FVIII relative to the phospholipid membrane. These residues were mutated to Cys in combination with masking of the Cys2000 following its mutation to Ser thereby yielding a single site for modification.

This above approach yielded a series of uniquely labeled FVIIIa molecules to utilize in FRET studies between a donor fluorophore molecule at a single site in the protein and OR molecules distributed on the PLV. Fig 1 shows binding titration results obtained for FVIIIa containing PyMPO-A3C1C2 (WT), fluorescein-A3C1C2 (Cys2000Ser/Asp1828Cys) and fluorescein-A3C1C2 (Cys2000Ser/Thr1872Cys) with OR-PLV as detected by FRET. Fluorescein was chosen for use with the mutants because of improved fluorescence sensitivity. The binding curves yielded hyperbolic patterns that were saturable. The estimated $K_d$ values, 3.4 ± 2.9, 5.0 ± 3.8, and 4.9 ± 1.6 nM, respectively, were equivalent to the value (3.2 ± 0.5 nM) reported previously using WT FVIII [11]. These results indicated that neither modification of the A3C1C2 subunit with the fluorophore nor the above mutations and subsequent reconstitution into FVIIIa appreciably affected the affinity of the

FVIIIa forms for the membrane. These data also indicated that FVIIIa was nearly saturated at PL > 20 μM. Thus, subsequent experiments to determine maximum energy transfer efficiency for distance measurements used 60 μM PL.

## Distance measurements between donor (PyMPO or fluorescein) and acceptor (OR) fluorophores by FRET

Reconstituted FVIIIa molecules having PyMPO (or fluorescein) bound to a single Cys residue at either residue 310, 692, 2000, 1828, or 1872 were subjected to FRET experiments to obtain $F/F_0$ where FVIIIa was saturated with PLV (60 μM PL). Asp1828 and Thr1872 in the A3 domain were selected for additional donor fluorophore labeling sites because these residues are located on the surface of A3 and away from the free Cys (Cys2000). To obtain A3C1C2 subunit with a single free Cys (at either Asp1828 or Thr1872), Cys2000 in WT A3 domain was mutated to Ser. Both FVIII variants with the double mutations (Cys2000Ser/Thr1872Cys and Cys2000Ser/Asp1828Cys) were expressed with minimal effects on cofactor activity (46–76% activity compared to WT FVIII by one-stage and two-stage assay, Table 1). These levels of FVIII activity are within the range for a normal FVIII phenotype. FRET experiments were performed using FVIIIa containing donor fluorophore in the A3C1C2 subunit at positions 2000, 1828, and 1872; the donor fluorophore A1 subunit at position 310, and donor fluorophore in A2 subunit at position 692.

Energy transfer parameter values (quantum yield, spectral overlap between donor fluorophore emission and OR absorption for all fluorophore sites) are listed in Table 2. This Table includes subsequently calculated $R_0$ values as well as anisotropy values. The geometric factor ($k^2$) used for the calculation of $R_0$ was typically assumed to be 2/3, which reflects freedom of rotation of donor and acceptor fluorophores. However, the anisotropy values for PyMPO were relatively high and this resulted in an increase in uncertainty of the $k^2$ value. However, because of the significantly low anisotropy (0.056) for the acceptor fluorophore (OR) it appeared reasonable to set the range of $R_0$ values as ±10% [29, 33]. Each $L$ value was determined after curve-fitting using data with various acceptor density values ($\sigma R_0^2$) and this is illustrated in Fig. 2A–B. It is unclear why the deviation from the fitted curve was more prominent at closer distances between donor and acceptor, and at higher OR density. However, since the correlation coefficient values for all fitted data were >0.94 and SD values were <10%, this deviation (if any) would be minor and should not affect final distant range values. The range of each $L$ value was similarly determined by using 10% reduced $R_0$ values or 10% increased $R_0$ values and is listed in Table 2. The standard deviation values for curve-fitting were <10% in all cases. Although there were some variations in quantum yield among donor fluorophore sites (up to an ~32% difference), the calculated $R_0$ values varied only ~5%. The $L$ values tended to be a little higher with the fluorescein-labeled group compared to the PyMPO-labeled group, likely reflecting the difference in status of the transition dipole (location and degree of rotational freedom).

## FVIIIa molecular orientation on a PLV surface

Based on the above distance measurements, all possible planes representing PLV surface orientation which satisfied the distance criteria ($L$ values) for all point data were initially

selected. In order to further exclude PLV planes with unlikely orientation we introduced the condition where both C1 and C2 domains contribute to PLV binding [7–10, 12, 13]. Following initial screening, PLV planes that were oriented near orthogonal (90° ± 10°) to the FVIII axis were selected (Fig. 3). Nearly 9000 possible PLV planes were finally selected and the results are shown in Fig. 4A–B. Figure 4A shows the distribution of the tilt angle values of the PLV planes against the FVIII axis (a line including the Cα atom of Pro505 and the N atom of Asn2172) shown in side view of FVIII (Fig. 4B). The minimum and maximum angles determined were 31.3° and 48.6°, respectively. The intersecting lines of these PLV planes with the FVIII axis plane are shown in red and blue dotted lines, respectively (Fig. 4B). Thus the possible PLV membrane surface exists within this tilt range relative to the FVIII axis. From this group of selected PLV planes, 94.3% fell within the angle value range of 34–46° while 76.5% fell within the angle value range of 36–42°. A representative PLV membrane plane obtained with an angle value of 38.5° is shown as a PLV membrane surface depicted by white spheres. This orientation shows a reduced distance between the three A domains and the PLV surface, and juxtaposes the A3 domain in close proximity to the surface. Thus residues contained within the latter domain may form direct contacts with the PLV.

### Binding of FVIII-A3 mutants to PLV by FRET

The above orientation of FVIII on PLV revealed that several regions in A3 domain appeared to be in contact with PLV. Fig. 5 shows the electrostatic potential map of FVIII. Viewing FVIII from the face contacting the PLV surface (bottom view) reveals an area in the A3 domain with significant positive charge (circled). This area is composed of Ser1713-Gly1725 and Arg1900-Pro1902 [3]. Since the positive charges in this region are derived from Arg1719, Arg1721, and Arg1900 we tested the possibility that these residues were involved in PLV binding. Individual charge reversal variants of FVIII were generated where Arg residues were replaced with Asp. FVIII Arg1719Asp and Arg1721Asp variants exhibited >50% wild type-like activity in both one-stage and two-stage assays (Table 1). The Arg1900Asp variant could not be expressed for reasons that are not clear. The two charge reversal variants were labeled with PyMPO. Labeling was performed using the intact FVIII thus the free Cys residues in each A domain were susceptible to modification. Binding of the labeled FVIII to variable concentrations of PLV was monitored by FRET as described in Methods. As shown in Fig. 6 both FVIII mutants bound to PLV showing saturable, hyperbolic patterns. The estimated $K_d$ values were 153.1 ± 42.6 nM and 188.9 ± 58.5 nM for the Arg1719Asp and Arg1721Asp FVIII variants, respectively. These values are ~48- and ~60-fold, respectively, larger than the $K_d$ value (3.2 ± 0.5 nM) reported previously using WT FVIII [11] and these differences correspond to losses in Gibbs free energy of 2.3 and 2.4 kcal/mol, respectively. While these mutations may result in a change in orientation, the observed loss in binding energy suggests that these two basic residues directly, or possibly indirectly, contribute to interaction with the membrane surface.

## DISCUSSION

In this report we present experimental evidence for the orientation of FVIIIa in relation to the PLV surface. Distance measurements obtained by FRET used PyMPO or fluorescein as

a donor fluorophore to label existing or created Cys residues in each isolated FVIIIa subunit. Labeled subunits were subsequently reconstituted with the unlabeled, complementary subunits to form the FVIIIa cofactor. Cys residues used for fluorophore modification included Cys310, Cys692, and Cys2000 in the A1, A2 and A3 domains, respectively. In addition, FVIII variants with the double mutation of Cys2000Ser/Asp1828Cys and Cys2000Ser/Thr1872Cys were generated to utilize Cys1828 and Cys1872 in the A3 domain for FRET. Distance measurements from these 5 positions in the protein to the PLV surface, labeled with the acceptor fluorophore OR, indicated that FVIIIa is oriented with a tilt ranging from 31.3–48.6° relative to the surface plane of the PLV. This orientation likely juxtaposes the A3 domain to close proximity with the membrane surface.

PLV binding regions in FVIII localize to the tips of the spikes in C1 and C2 domains, which include Lys2092-Phe2093, Gln2042-Tyr2043, and Arg2159 on C1 [12, 13], and Leu2251-Leu2252, Met2199-Phe2200, Lys2227, and Trp2313-His2315 on C2 [7–10]. Thus both C1 and C2 domains likely contribute to PLV binding. Therefore, a true PLV plane should be at a near level position in the conventional front view and we utilized this condition to exclude any PLV planes with unrealistic orientations. This assumption was necessary because our data does not exclude unrealistic planes due to the fact that the 5 Cys locations in FVIII used for distance measurements are in close proximity in the front view (Fig. 3). Subsequently we could select PLV planes with a small variation in the range of angles with the FVIII axis (31.3–48.6°) in the side view due in part to the use of two different donor fluorophores with different *L* values at the same Cys site.

While the X-ray structure of FVIII [3] (PDB#3CDZ) we utilized in our model is of intermediate resolution (~4 Å), the relative coordinates of residues Cys310, Cys692, Cys2000, Asp1828, and Thr1872 are likely accurate since these coordinates are quite similar to the ones in another intermediate resolution FVIII X-ray crystal structure described by Shen *et al.* [2] (PDB#2R7E). Furthermore, the coordinates of Cys310 and Cys2000 comprise parts of type I copper sites in the A1 and A3 domains, respectively, of FVIII and for this reason are considered to be more accurate because of the reliability of assignment of metal ion sites.

The molecular orientation of FVIIIa on the PLV surface we describe in this report is in good agreement with the orientation of FVIII on PLV previously proposed by Ngo *et al* [3] in a model docking FVIII to FIXa on the PLV surface. In that model, the authors performed FVIIIa-FIXa docking calculations based upon several known interactive sites in the two proteins. This information was used in conjunction with earlier FRET results [29] that used a donor fluorophore labeled in the active site of FIXa and acceptor fluorophores distributed on the PLV to determine that the FIXa active site was located 75 – 80 Å above the membrane surface. The resultant model of the membrane bound FVIII-FIXa complex yielded a tilt to the FVIII protein, which positions the A3 domain close to the membrane surface. Although the coordinates of the membrane are not listed in that report, the tilt angle seems to fall in the range of angle we obtained (31.3–48.6°).

The orientation of FVIIIa on the membrane surface we propose is supported by known PLV-interactive sites in the protein and importantly, suggests other potential interactive sites.

Rigorous structural information on the FVIII-PLV interaction is limited. A recent study (10) reported a high resolution X-ray crystal structure for a small molecule inhibitor of the FVIII-PLV interaction bound to the C2 domain. These authors showed the inhibitor bound to residues Trp2313-His2315, which is localized to the PLV-interactive surface in the model described in the current report. Furthermore, we note that there is a relatively large area rich in basic residues contained in the A3 domain that is likely in contact with the PLV surface (see Fig. 5, bottom view). One of these regions, Ser1713-Gly1725, contains residues Arg1719 and Arg1721 that are not defined in the intermediate resolution X-ray structures. However, we show that charge reversal point mutations (Arg to Asp) at these residues resulted in marked increases in $K_d$ values consistent with an electrostatic interaction of these basic residues with the polar head groups of PS. Interestingly, FIXa and FXa inefficiently cleave FVIII LC at Arg1719 or Arg1721, respectively [34, 35] as compared with other cleavage sites in the cofactor, e. g. Arg336. One reason for this slow cleavage rate may reflect partial masking of the site(s) by PLV, which is a necessary component for cleavage of FVIII substrates by these proteinases. In addition, regions defined by Arg2033-Gln2045 in the C1 domain and Gln2276-Lys2281 in the C2 domain that show a high density basic as well as hydrophobic residues are located at the PLV binding surface in FVIII (see Fig. 5, bottom view). Although no experimental evidence exists for residues within these sequences as contributing to interaction with PLV, their presence warrants further investigation.

The present model showing FVIII associated with a rigid flat plane representing the PLV surface does not perfectly accommodate all regions in the A3, C1, and C2 domains proposed to contact the PLV surface. Additional mechanisms such as conformational changes particularly at inter-domain interfaces (A3-C1, A1-C2 and so on), burial of relatively large area of FVIII into the phospholipid bilayer (C1 and C2), and/or local bends in the PLV surface may resolve these discrepancies. Immersion of basic or hydrophobic groups into the lipid membrane is not uncommon [36, 37]. For example, Majumder e*t al* experimentally confirmed a deep penetration of Trp2063/Trp2064 indole moieties of FVa into the lipid bilayer (~9 Å from the center of lipid bilayer, total length of acyl group is ~15 Å) [37]. Furthermore, residues selected for labeling with donor fluorophores include Cys310, Cys692, and Cys2000, which contain a free thiol for facile labeling yet appear to be partially buried according to the FVIII structure [3]. Although the labeled FVIII proteins retained high specific activity, labeling at these sites might have some impact on the surrounding structure possibly affecting orientation. We note that reduced quantum yield and increased anisotropy values were observed when PyMPO was used as a fluorescence donor. These characteristics are undesirable in estimating spatial separations by FRET as they lead to increased uncertainty in $R_0$ and $k^2$ parameters, respectively. Thus further investigations using alternate probe sites with additional fluorophores may be necessary to more rigorously determine the membrane-bound orientation.

In conclusion, results presented in this report provide experimental evidence for the molecular orientation of FVIIIa on a membane surface. Data from multiple FRET pairings indicate a defined tilt to the protein relative to surface. Further experiments are required to refine this model and to assess new, potential interactive sites suggested by the model.

## Acknowledgments

We thank Lisa M. Regan of Bayer Corporation for the gifts of recombinant human FVIII, and Pete Lollar and John Healey for the FVIII cloning and expression vectors.

**FUNDING**

This work was supported by NIH grants HL38199 and HL76213.

## The abbreviations used are

| | |
|---|---|
| **FVIII** | factor VIII |
| **FVIIIa** | factor VIIIa |
| **HC** | heavy chain |
| **LC** | light chain |
| **FIXa** | factor IXa |
| **FX** | factor X |
| **FXase** | factor Xase |
| **PC** | phosphatidylcholine |
| **PE** | phosphatidylethanolamine |
| **PS** | phosphatidylserine |

## References

1. Fay PJ. Activation of factor VIII and mechanisms of cofactor action. Blood Rev. 2004; 18:1–15. [PubMed: 14684146]
2. Shen BW, Spiegel PC, Chang CH, Huh JW, Lee JS, Kim J, Kim YH, Stoddard BL. The tertiary structure and domain organization of coagulation factor VIII. Blood. 2008; 111:1240–1247. [PubMed: 17965321]
3. Ngo JC, Huang M, Roth DA, Furie BC, Furie B. Crystal structure of human factor VIII: implications for the formation of the factor IXa-factor VIIIa complex. Structure. 2008; 16:597–606. [PubMed: 18400180]
4. Gilbert GE, Arena AA. Activation of the factor VIIIa-factor IXa enzyme complex of blood coagulation by membranes containing phosphatidyl-L-serine. J Biol Chem. 1996; 271:11120–11125. [PubMed: 8626656]
5. Gilbert GE, Drinkwater D. Specific membrane binding of factor VIII is mediated by O-phospho-L-serine, a moiety of phosphatidylserine. Biochemistry. 1993; 32:9577–9585. [PubMed: 8373765]
6. Novakovic VA, Cullinan DB, Wakabayashi H, Fay PJ, Baleja JD, Gilbert GE. Membrane-binding properties of the Factor VIII C2 domain. Biochem J. 2011; 435:187–196. [PubMed: 21210768]
7. Gilbert GE, Kaufman RJ, Arena AA, Miao H, Pipe SW. Four hydrophobic amino acids of the factor VIII C2 domain are constituents of both the membrane-binding and von Willebrand factor-binding motifs. J Biol Chem. 2002; 277:6374–6381. [PubMed: 11698391]
8. Lewis DA, Pound ML, Ortel TL. Contributions of Asn2198, Met2199, and Phe2200 in the factor VIII C2 domain to cofactor activity, phospholipid-binding, and von Willebrand factor-binding. Thromb Haemost. 2003; 89:795–802. [PubMed: 12719775]
9. Pellequer JL, Chen SW, Saboulard D, Delcourt M, Negrier C, Plantier JL. Functional mapping of factor VIII C2 domain. Thromb Haemost. 2011; 106:121–131. [PubMed: 21614407]

10. Liu Z, Lin L, Yuan C, Nicolaes GA, Chen L, Meehan EJ, Furie B, Furie B, Huang M. Trp2313-His2315 of factor VIII C2 domain is involved in membrane binding: structure of a complex between the C2 domain and an inhibitor of membrane binding. J Biol Chem. 2010; 285:8824–8829. [PubMed: 20089867]
11. Wakabayashi H, Griffiths AE, Fay PJ. Factor VIII lacking the C2 domain retains cofactor activity in vitro. J Biol Chem. 2010; 285:25176–25184. [PubMed: 20529839]
12. Meems H, Meijer AB, Cullinan DB, Mertens K, Gilbert GE. Factor VIII C1 domain residues Lys 2092 and Phe 2093 contribute to membrane binding and cofactor activity. Blood. 2009; 114:3938–3946. [PubMed: 19687511]
13. Lu J, Pipe SW, Miao H, Jacquemin M, Gilbert GE. A membrane-interactive surface on the factor VIII C1 domain cooperates with the C2 domain for cofactor function. Blood. 2011; 117:3181–3189. [PubMed: 21156843]
14. Peng W, Quinn-Allen MA, Kane WH. Mutation of hydrophobic residues in the factor Va C1 and C2 domains blocks membrane-dependent prothrombin activation. J Thromb Haemost. 2005; 3:351–354. [PubMed: 15670043]
15. Saleh M, Peng W, Quinn-Allen MA, Macedo-Ribeiro S, Fuentes-Prior P, Bode W, Kane WH. The factor V C1 domain is involved in membrane binding: identification of functionally important amino acid residues within the C1 domain of factor V using alanine scanning mutagenesis. Thromb Haemost. 2004; 91:16–27. [PubMed: 14691564]
16. Peng W, Quinn-Allen MA, Kim SW, Alexander KA, Kane WH. Trp2063 and Trp2064 in the factor Va C2 domain are required for high-affinity binding to phospholipid membranes but not for assembly of the prothrombinase complex. Biochemistry. 2004; 43:4385–4393. [PubMed: 15065883]
17. Doering C, Parker ET, Healey JF, Craddock HN, Barrow RT, Lollar P. Expression and characterization of recombinant murine factor VIII. Thromb Haemost. 2002; 88:450–458. [PubMed: 12353075]
18. Wakabayashi H, Freas J, Zhou Q, Fay PJ. Residues 110-126 in the A1 domain of factor VIII contain a Ca2+ binding site required for cofactor activity. J Biol Chem. 2004; 279:12677–12684. [PubMed: 14722121]
19. Fay PJ, Smudzin TM. Characterization of the interaction between the A2 subunit and A1/A3-C1-C2 dimer in human factor VIIIa. J Biol Chem. 1992; 267:13246–13250. [PubMed: 1618828]
20. Wakabayashi H, Su YC, Ahmad SS, Walsh PN, Fay PJ. A Glu113Ala Mutation within a Factor VIII Ca(2+)-Binding Site Enhances Cofactor Interactions in Factor Xase. Biochemistry. 2005; 44:10298–10304. [PubMed: 16042406]
21. Over J. Methodology of the one-stage assay of Factor VIII (VIII:C). Scand J Haematol Suppl. 1984; 41:13–24. [PubMed: 6440279]
22. Lollar P, Fay PJ, Fass DN. Factor VIII and factor VIIIa. Methods Enzymol. 1993; 222:128–143. [PubMed: 8412790]
23. Wakabayashi H, Koszelak ME, Mastri M, Fay PJ. Metal ion-independent association of factor VIII subunits and the roles of calcium and copper ions for cofactor activity and inter-subunit affinity. Biochemistry. 2001; 40:10293–10300. [PubMed: 11513607]
24. Wakabayashi H, Schmidt KM, Fay PJ. Ca(2+) binding to both the heavy and light chains of factor VIII is required for cofactor activity. Biochemistry. 2002; 41:8485–8492. [PubMed: 12081499]
25. Mimms LT, Zampighi G, Nozaki Y, Tanford C, Reynolds JA. Phospholipid vesicle formation and transmembrane protein incorporation using octyl glucoside. Biochemistry. 1981; 20:833–840. [PubMed: 7213617]
26. Chen PS, Toribara TY, Warner H. Microdetermination of Phosphorus. Anal Chem. 1956; 28:1756–1758.
27. Yegneswaran S, Wood GM, Esmon CT, Johnson AE. Protein S alters the active site location of activated protein C above the membrane surface. A fluorescence resonance energy transfer study of topography. J Biol Chem. 1997; 272:25013–25021. [PubMed: 9312108]
28. Marsh DJ, Lowey S. Fluorescence energey transfer in myosin subfragment-1. Biochemistry. 1980; 19:774–784. [PubMed: 6444519]

29. Mutucumarana VP, Duffy EJ, Lollar P, Johnson AE. The active site of factor IXa is located far above the membrane surface and its conformation is altered upon association with factor VIIIa. A fluorescence study. J Biol Chem. 1992; 267:17012–17021. [PubMed: 1512240]
30. Magde D, Wong R, Seybold PG. Fluorescence quantum yields and their relation to lifetimes of rhodamine 6G and fluorescein in nine solvents: improved absolute standards for quantum yields. Photochem Photobiol. 2002; 75:327–334. [PubMed: 12003120]
31. Shaklai N, Yguerabide J, Ranney HM. Interaction of hemoglobin with red blood cell membranes as shown by a fluorescent chromophore. Biochemistry. 1977; 16:5585–5592. [PubMed: 921951]
32. Cerione RA, McCarty RE, Hammes GG. Spatial relationships between specific sites on reconstituted chloroplast proton adenosinetriphosphatase and the phospholipid vesicle surface. Biochemistry. 1983; 22:769–776. [PubMed: 6220736]
33. Fung BK, Stryer L. Surface density determination in membranes by fluorescence energy transfer. Biochemistry. 1978; 17:5241–5248. [PubMed: 728398]
34. O'Brien DP, Johnson D, Byfield P, Tuddenham EG. Inactivation of factor VIII by factor IXa. Biochemistry. 1992; 31:2805–2812. [PubMed: 1547220]
35. Eaton D, Rodriguez H, Vehar GA. Proteolytic processing of human factor VIII. Correlation of specific cleavages by thrombin, factor Xa, and activated protein C with activation and inactivation of factor VIII coagulant activity. Biochemistry. 1986; 25:505–512. [PubMed: 3082357]
36. Pellequer JL, Gale AJ, Griffin JH, Getzoff ED. Homology models of the C domains of blood coagulation factors V and VIII: a proposed membrane binding mode for FV and FVIII C2 domains. Blood Cells Mol Dis. 1998; 24:448–461. [PubMed: 9880241]
37. Majumder R, Quinn-Allen MA, Kane WH, Lentz BR. The phosphatidylserine binding site of the factor Va C2 domain accounts for membrane binding but does not contribute to the assembly or activity of a human factor Xa-factor Va complex. Biochemistry. 2005; 44:711–718. [PubMed: 15641797]

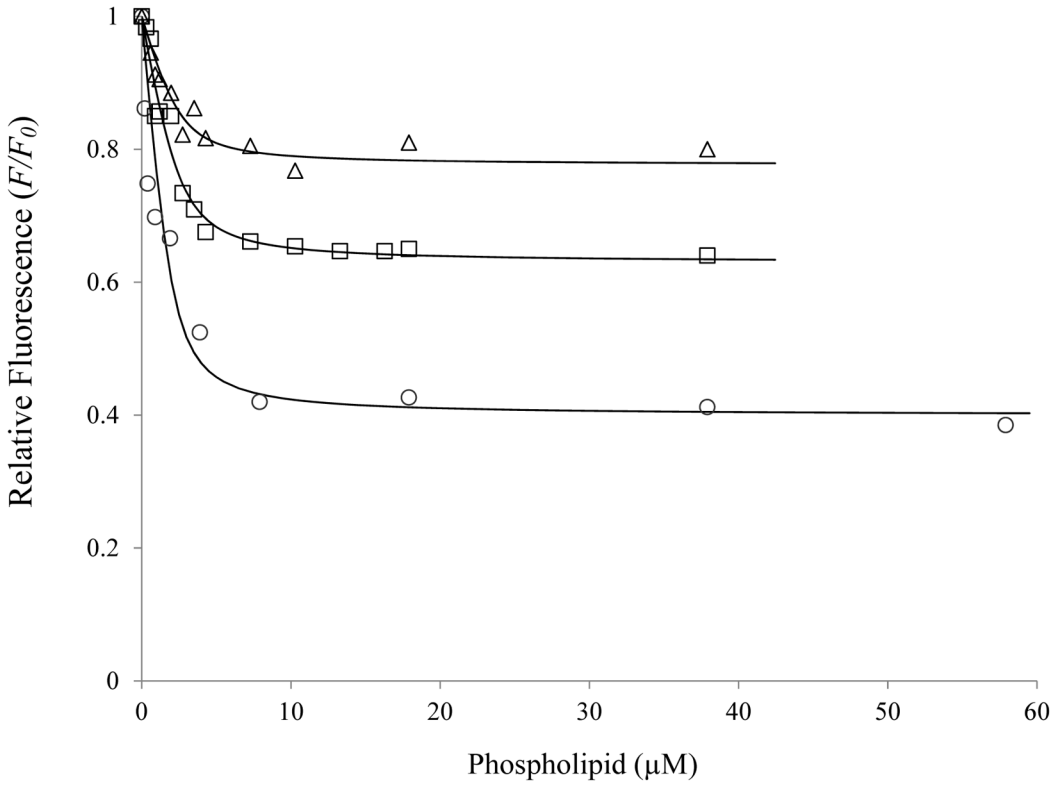


**Figure 1. Binding of PyMPO-A3C1C2 (WT) or fluorescein-A3C1C2 (mutants) reconstituted with A1 and A2 subunit to PLV detected by FRET**

FVIIIa reconstituted from 20 nM PyMPO (or fluorescein)-A3C1C2, 1 μM A1, and 400 nM A2 in HEPES buffer containing 300 μM PC vesicles was titrated with 0- 58 μM (or 0–38 μM) PLV containing OR and emission at 540–546 nm (PyMPO, 417 nm excitation) or 520–526 (fluorescein, 495 nm excitation) was monitored as described in Methods. $F_0$ is the fluorescence intensity of the sample titrated with unlabeled phospholipid. $F$ is the corrected fluorescence intensity of the sample titrated with phospholipid vesicles containing OR. The acceptor density was $4.7 \times 10^{-4}$ OR molecules/Å$^2$. Data were fitted to an equilibrium binding equation by non-linear least squares regression as described in Methods and lines were drawn. Data points for WT (circles), Cys2000Ser/Asp1828Cys (triangles) and Cys2000Ser/Thr1872Cys (squares) represent the average of 3 determinations.

Fig. 2A

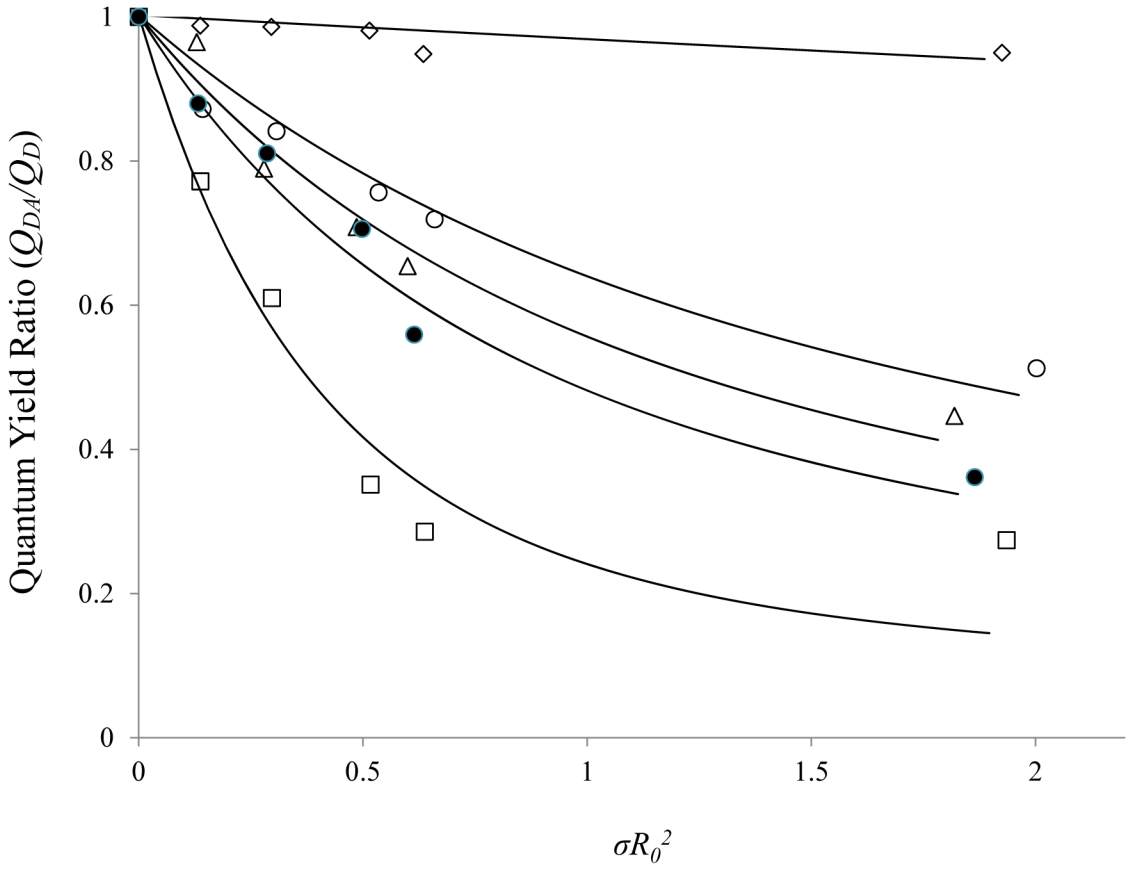

Fig. 2B

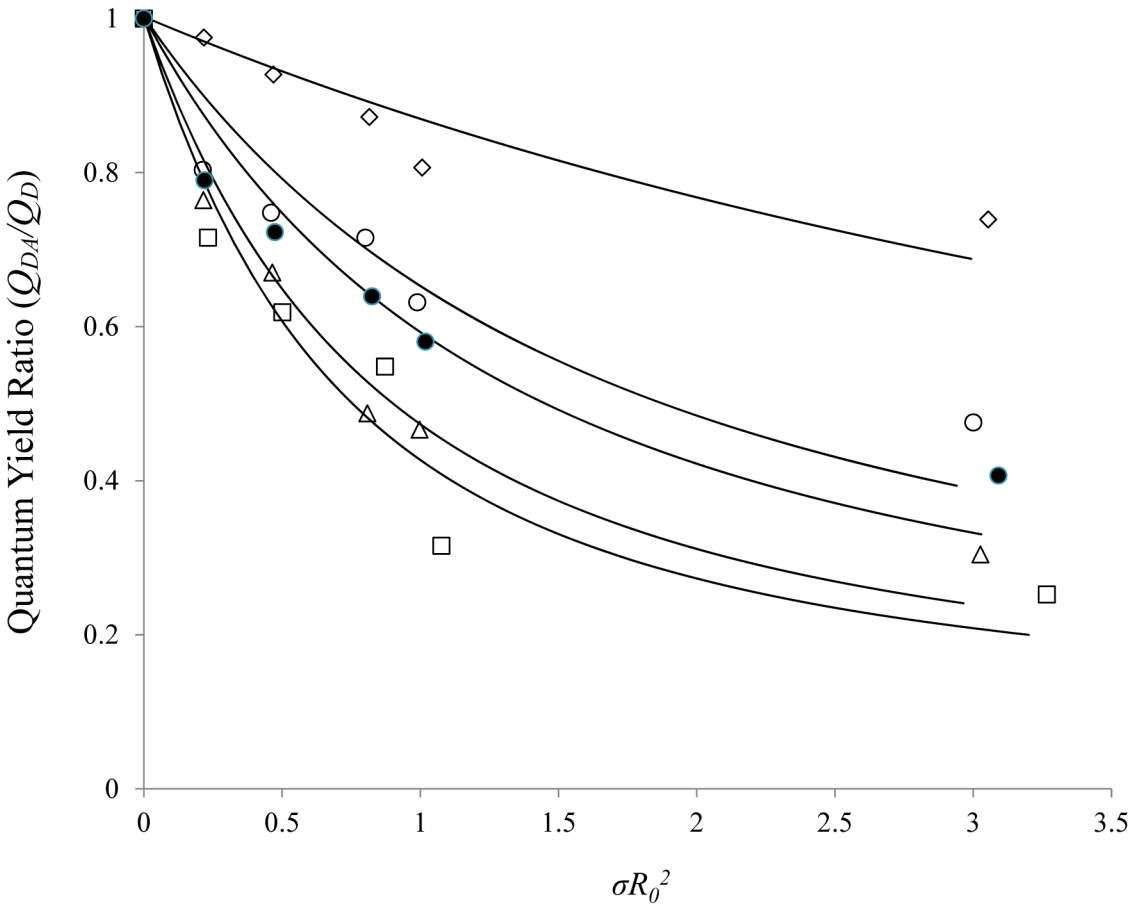


**Figure 2. Energy transfer efficiency (quantum yield ratio) as a function of acceptor density ($\sigma R_0^2$)**

FVIIIa reconstituted from 50 nM PyMPO- (A) or fluorescein- (B) labeled subunits with excess subunits (400–1000 nM) in HEPES buffer containing 300 μM PC vesicles was titrated with 60 μM PLV containing OR with various density and emission at 540–546 nm (PyMPO, 417 nm excitation) or 520–526 (fluorescein, 495 nm excitation) was monitored. The values of $Q_{DA}/Q_D$, the ratio of donor quantum yield in the sample with OR-labeled and unlabeled PLV and given by the ratio of the corrected fluorescence intensity of the samples with OR-labeled and unlabeled PLV ($=F/F_0$) were determined. Using $R_0$ as listed in Table 2 the distance of closest approach ($L$) between PyMPO- (A) or fluorescein- (B) labeled subunits and OR-PLV was obtained by nonlinear least-squares regression as described in the Methods and lines were drawn. Data points for donor-fluorophore-labeled A1 (open circles), A2 (open triangles), A3C1C2 (open squares), Cys2000Ser/Asp1828Cys A3C1C2 (open diamonds) and Cys2000Ser/Thr1872Cys A3C1C2 (closed circles) represent the average of 3 determinations.

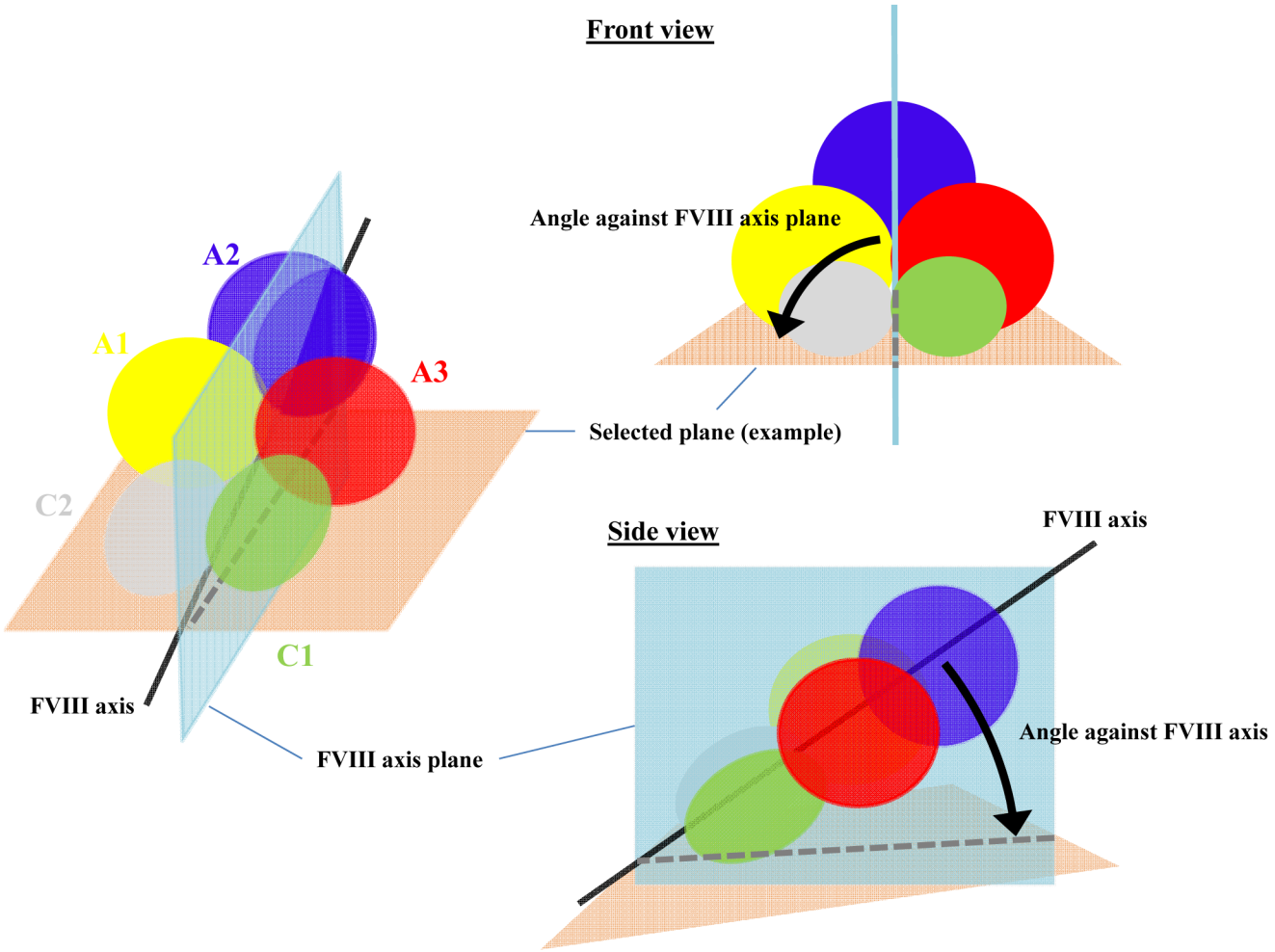


**Figure 3. Definition of planes and angles**

The transparent light blue plane represents the FVIII axis plane which is defined by 3 atoms (N of Gly458, Cα of Ser313, and N of Asn2172) and is positioned approximately vertically. A FVIII axis, shown as a line including the Cα atom of Pro505 and N atom of Asn2172, is nearly on the FVIII axis plane. An angle formed by a selected plane (transparent orange plane) and the FVIII axis plane is shown in the front view and an angle formed by a selected plane and FVIII axis is shown in the side view. A1 (yellow), A2 (blue), A3 (red), C1 (green), and C2 (grey) subunits are depicted as spheres.

Fig. 4A

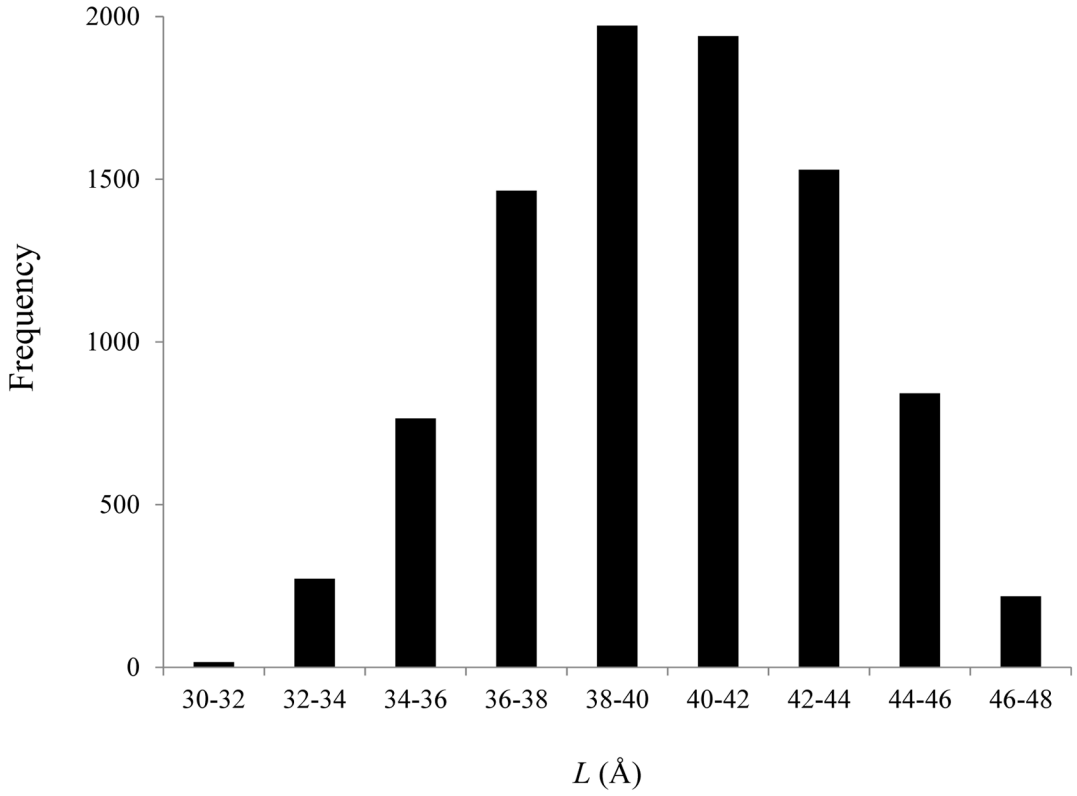

Fig. 4B

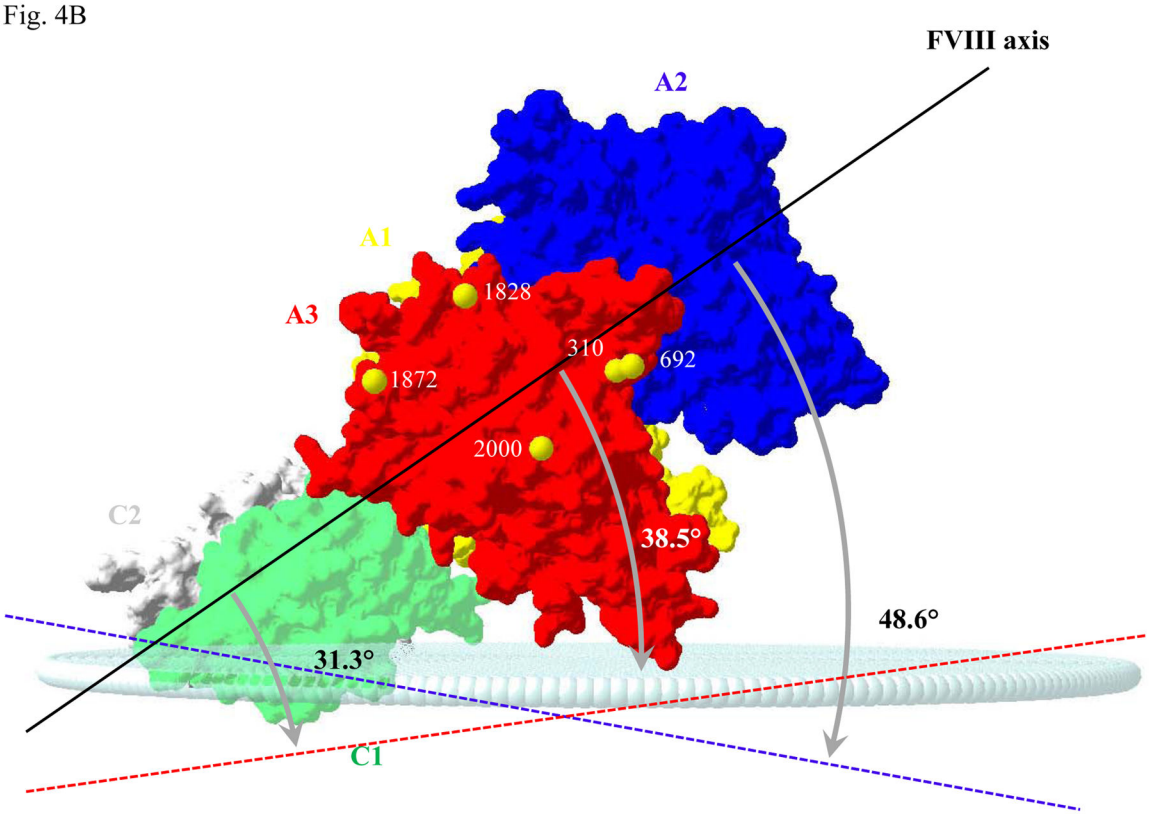


**Figure 4.**

**(A) Histogram of FVIII tilt angle value distribution of selected planes relative to the PLV membrane surface** Based on the data from the distance of closest approach (*L*) for each Cys location possible planes were selected as described in Methods and the distribution of angle values between selected planes and FVIII axis were calculated.

**(B) FVIII orientation on the PLV surface** FVIII domain surfaces based on the X-ray crystal structure are calculated and drawn by Swiss PDB viewer (probe size = 1.4 Å) as colored by yellow (A1), blue (A2), red (A3), green (C1), and C2 (gray). The intersecting lines of FVIII axis plane with a PLV plane that forms a minimum angle (31.3°) and a PLV plane that forms a maximum angle (48.6°) are shown as red and blue dotted lines, respectively. An example of a PLV membrane plane obtained with an angle value of 38.5° is shown as white spheres (0.225x + 0.974y + 0.035z + 6.60 = 0 in Cartesian coordinates in FVIII structure file) [3]. Sulfur atoms for each Cys residues were depicted as yellow spheres.

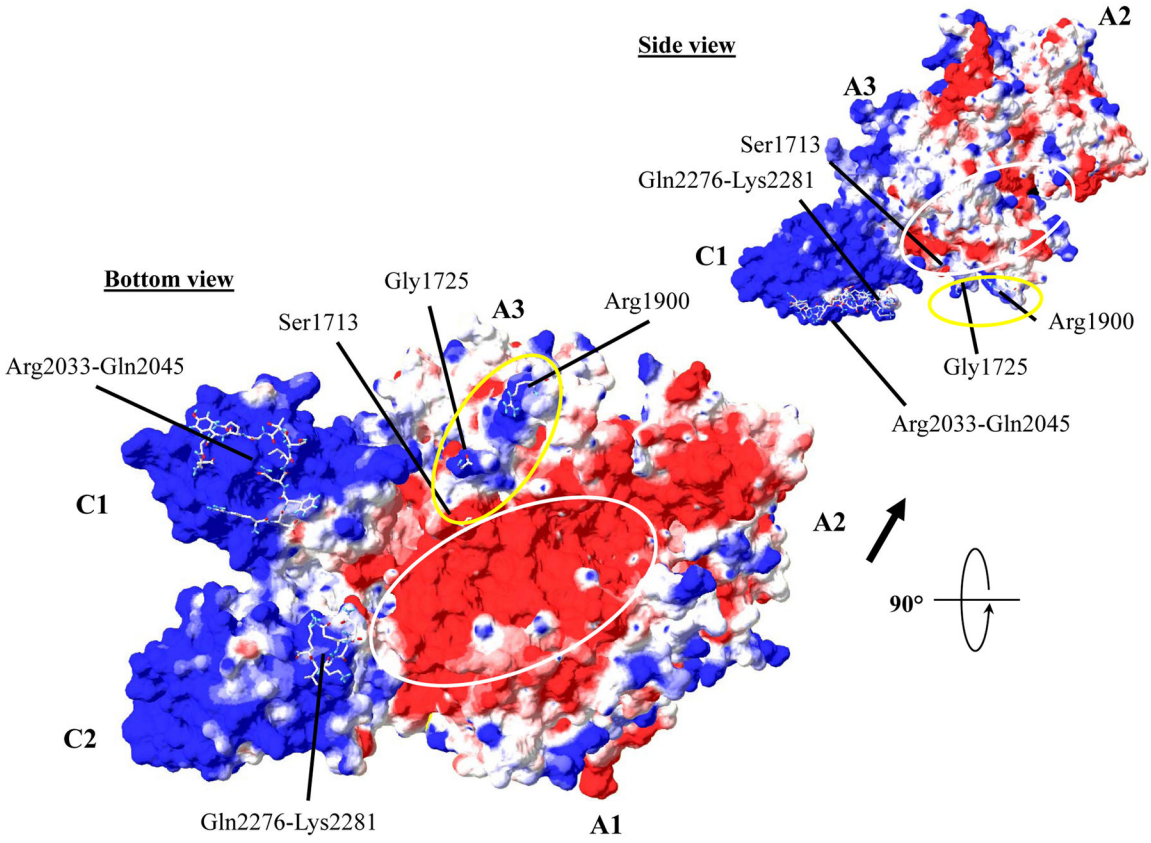


**Figure 5. Electrostatic potential distribution on the FVIII surface (probe size = 1.4 Å)**

Electrostatic potential was calculated by Swiss PDB viewer with a simple coulomb interaction mode using a uniform dielectric constant (= 80) and shown as red (negative) and blue (positive). A large acidic region in the middle of the 'back' of FVIII is marked as a white circle. The area circled in yellow corresponds to a basic region composed of Arg1719, Arg1721, and Arg1900. Several residues on A3, C1 and C2 subunits are drawn in stick representations.

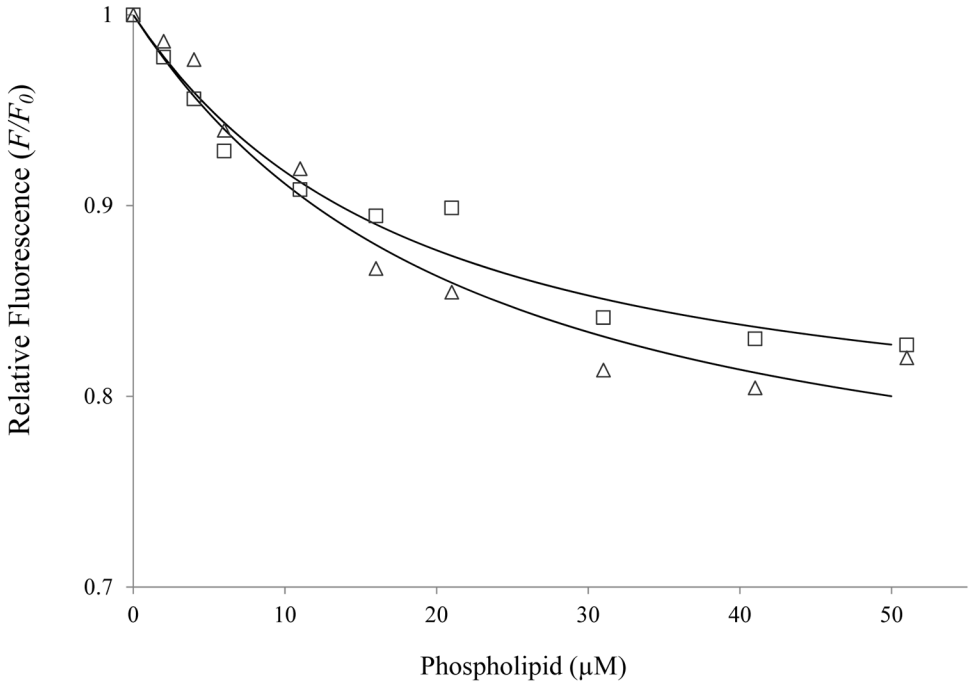


**Figure 6. Binding of PyMPO-FVIII mutants to PLV detected by FRET**

PyMPO-labeled Arg1719Asp FVIII (40 nM; triangles) and Arg1719Asp FVIII (40 nM; squares) in HEPES buffer containing 300 μM PC vesicles were titrated with phospholipid vesicles containing OR and emission at 540–546 nm was monitored as described in Methods. $F_0$ is the fluorescence intensity of the sample titrated with unlabeled phospholipid. $F$ is the corrected fluorescence intensity of the sample titrated with phospholipid vesicles containing OR. The acceptor density was $4.7 \times 10^{-4}$ OR molecules/Å$^2$. Data were fitted to an equilibrium binding equation by non-linear least squares regression as described in Methods and lines were drawn.

## Table 1

Specific activity of FVIII mutants

| FVIII variant | One-stage clotting assay (Unit/μg) | Two-stage FXa generation assay (nM FXa generated/min/nM FIXa) |
|---|---|---|
| WT | 4.50 ± 0.60 (1.00) | 196.7 ± 7.9 (1.00) |
| Cys2000Ser/Asp1828Cys | 2.49 ± 0.09 (0.55) | 144.2 ± 2.5 (0.73) |
| Cys2000Ser/Thr1872Cys | 2.06 ± 0.06 (0.46) | 149.8 ± 1.1 (0.76) |
| Arg1719Asp | 3.76 ± 0.42 (0.84) | 125.9 ± 1.9 (0.64) |
| Arg1721Asp | 3.15 ± 0.24 (0.70) | 99.7 ± 0.2 (0.51) |

Specific activity was determined by one-stage clotting assay and by FXa generation assay where FIXa was saturated with each FVIII variant as described in Methods. Data represents average values and standard deviations from three separate determinations. Values in parentheses are relative to the WT value.

**Table 2**

Energy transfer parameters and the distance ($L$) of closest approach

| | Quantum yield | Spectral overlap | Anisotropy | $R_0$ (Å) | $L$ (Å) |
|---|---|---|---|---|---|
| PyMPO-A1 | 0.064 | $1.23 \times 10^{15}$ | 0.34 | 33.7 | 33.1 – 44.9 |
| PyMPO-A2 | 0.048 | $1.22 \times 10^{15}$ | 0.34 | 32.1 | 29.7 – 40.4 |
| PyMPO-A3C1C2 | 0.056 | $1.26 \times 10^{15}$ | 0.33 | 33.2 | 16.7 – 27.5 |
| PyMPO-1828 | 0.058 | $1.20 \times 10^{15}$ | 0.32 | 33.1 | 54.0 – 68.0 |
| PyMPO-1872 | 0.053 | $1.20 \times 10^{15}$ | 0.33 | 32.5 | 27.2 – 37.6 |
| fl-A1 | 0.22 | $1.20 \times 10^{15}$ | 0.22 | 41.3 | 43.9 – 57.0 |
| fl-A2 | 0.24 | $1.13 \times 10^{15}$ | 0.18 | 41.5 | 34.6 – 47.6 |
| fl-A3C1C2 | 0.29 | $1.19 \times 10^{15}$ | 0.19 | 43.1 | 33.7 – 47.0 |
| fl-1828 | 0.25 | $1.13 \times 10^{15}$ | 0.19 | 41.7 | 56.4 – 73.5 |
| fl-1872 | 0.25 | $1.14 \times 10^{15}$ | 0.19 | 41.9 | 39.0 – 53.1 |
| OR-PLV | N/A | N/A | 0.056 | N/A | N/A |

FRET analysis using FVIIIa reconstituted from a PyMPO (or fluorescein)-labeled subunit combined with an excess concentration of unlabeled subunits and OR-labeled PLV was performed and distance of closest approach values ($L$) were calculated by nonlinear least square regression as described in Methods. Data represent average values from three separate determinations.